

Dynamic Response of Sandwich Plates Subjected to Impact Loading

K. S. Numayr¹⁾ and H. M. Dwairi¹⁾

¹⁾ Civil Engineering Department, Jordan University of Science and Technology, P.O. Box 3030, 22110, Irbid, Jordan, E-mail: numayr@just.edu.jo

ABSTRACT

Two models of three-layered sandwich plate are proposed in this paper to study the dynamic response of these types of plates when subjected to impact loading. Transverse shear and normal deformations are accounted for in the core, while the face layers are treated as thin plates. In the first model, the core is modeled as translational and rotational elastic springs connecting the face layers together and in plane displacements at the middle surface of the face layers are neglected, while in the second model the in plane displacements and shear stresses at the junctions of the face layers with the core are considered. The governing equations of motion are analytically solved to obtain a closed form solution for simply supported plates using the modal superposition method. The effects of various geometric and material parameters on the dynamic properties and response of sandwich plates are investigated. The present study results are compared with those obtained from the literature and are found to be in good agreement in most cases. It was shown in this study that the in plane displacements of the middle surface of face layers could be neglected for sandwich plates with thick or flexible core.

KEYWORDS: Sandwich plate, Impact, Response, Vibration, Modeling.

INTRODUCTION

The term "sandwich plate" here refers to a structure in the form of lightweight core with thin laminates bonded to each side of it. Today, interest of sandwich plates is growing steadily, since it offers the possibility of achieving high bending stiffness with small weight penalty. High quality composite laminates and filler materials could be easily manufactured for many applications. In the ship building industry in particular, the use of sandwich plates is well established. Small and very fast passenger vessels have for many years been built in sandwich materials. Especially for navy vessels and mine sweepers, the sandwich construction provides

some additional advantages. The use of sandwich plates for construction of railroad cars and other means of transportation is also widely considered today. More recently, sandwich construction was further applied in building primary structures of aircraft such as the wing's skin and the vertical fin torque box.

Many researchers investigated the impact problem of sandwich plates. Hoff (1950) presented a solution for the differential equations and associated boundary conditions for the bending and buckling problem of sandwich plates. The effect of shear deformation in the core was considered, while the effect of normal deformation was neglected. In 1972, Yan and Dowell (1972) presented a solution to a simple form of the differential equation of equilibrium for non-symmetric sandwich plates or beams made of isotropic and

Accepted for Publication on 15/7/2010.

homogeneous layers. Equal importance was given to both shear and bending effects of the sandwich, in the equations deduced. In 1982, Grover and Kapur (1982) studied the transient response of simply supported three layer visco-elastically damped sandwich plates, subjected to a half sine shock impulse. Only transverse inertia effects were considered. The properties of the visco-elastic core material have been represented by four-element visco-elastic model. Koller (1986) investigated the elastic impact of spheres on sandwich plates. In his study, a special sandwich plate theory was developed, which included bending of the facing sheets and transverse shear of the core, under the assumption of Hertzian contact. A Laplace transform was carried out on the equations of motion and was solved in transform space. In 1986, Sayir and Koller (1986) discussed the physical behavior of bending waves in sandwich plates in which the facings are thin, stiff and heavy as compared with the core, by means of asymptotic expansions of the basic equations of linear elasticity. Poltorak and Nagaya (1986) extended on the case of forced steady state vibration of Yan and Dowell (1972) equation of motion of sandwich plates or beams. The exact general solution of this equation is founded in terms of Bessel's functions, where the boundary conditions along the irregular edges are satisfied directly by means of the Fourier Expansion Collection Method. In 1988, He and Ma (1988) derived a set of simplified governing equations and the corresponding boundary condition of visco-elastically damped unsymmetrical sandwich plates in flexural vibration. An asymptotic solution of the simplified governing equations has been introduced, with the loss factor of the visco-elastic material of the core used as a parameter. Lee *et al.* (1993) studied the response of a sandwich plate impacted by a rigid ball using a sandwich theory, which modeled the face sheets as separate Mindlin plates with a core that transmits transverse shear as well as transverse normal

deformations. They used the Finite Element Method (FEM) to solve the equations of motion for the plate and impactor with a contact power law which was determined from static indentation tests. Lee and Kim (1997) investigated the effect of including normal deformation as well as shear deformation of the core layer on the modal property estimations of sandwich plates. Equations of motion were formulated by applying Hamilton's principle. The equations consist of two-coupled sixth order equations in terms of the transverse displacements. Lange and Bottega (1998) employed the exact solution by Bottega (1988) to investigate the transient axi-symmetric dynamic response of layered plates to impact loading.

In this study, the dynamic response of sandwich plates, with different geometric and material parameters and impact loading, is investigated. Equations of motion are derived using two simple mechanical models. The core is modeled as translational and rotational springs. Effects of normal and shear deformations are included using the mentioned types of springs. In the first model, the membrane displacements at the middle surface of the face layers are neglected, while in the second model those displacements are included. The effect of various geometric, material and impact loading type are investigated.

EQUATIONS OF MOTION

The coordinates and geometry of a rectangular sandwich plate, which has a visco-elastic core between two elastic plates, are shown in Figure (1). The following assumptions are made to derive the governing equations of motion: (1) Top and bottom layers are isotropic and homogeneous. (2) A normal straight line to the middle plane of the face layers before bending, remains straight and normal to the middle plane after bending; i.e. transverse shear deformation of the face layers is neglected. (3) Neglecting damping properties of the visco-elastic core. (4) There is a perfect

continuity at the interfaces and no slippage occurs while the plate is bending; i.e. displacements keep continuity at the inter-faces between the elastic plates and the visco-elastic core. (5) Inertia effects are considered in the transverse direction only; i.e. in-plane rotational accelerations are neglected. (6) The normal stresses σ_x , σ_y and in plane shear stresses τ_{xy} in the core are neglected, since the modulus of elasticity and shear modulus of the core are very small as compared with those of the face layers. (7) The thickness of the face layers is small in comparison with the plate dimensions ($L/h > 10$). (8) Small deformations are assumed and

nonlinear terms of strain-displacement relationships are neglected.

Consider infinitesimal elements of area ($dx \ dy$) in the upper and lower layers as shown in Figures (2), (3a) and (3b). The moments and forces acting on the two differential elements are shown in these figures where the upper infinitesimal element is subjected to a general transverse forcing function $P(x,y,t)$. Equilibrium of forces in the z-direction and moments about x and y-axes lead to the following moment equilibrium equations of the lower and upper layers, respectively:

$$\frac{\partial^2 m_x^{(1)}}{\partial x^2} + 2 \frac{\partial^2 m_{xy}^{(1)}}{\partial x \partial y} + \frac{\partial^2 m_y^{(1)}}{\partial y^2} + \frac{\partial M_x^{(1)}}{\partial x} + \frac{\partial M_y^{(1)}}{\partial y} + K_s (w_2 - w_1) - \bar{m}_1 \frac{\partial^2 w_1}{\partial t^2} = 0 \quad (1)$$

$$\frac{\partial^2 m_x^{(2)}}{\partial x^2} + 2 \frac{\partial^2 m_{xy}^{(2)}}{\partial x \partial y} + \frac{\partial^2 m_y^{(2)}}{\partial y^2} + \frac{\partial M_x^{(2)}}{\partial x} + \frac{\partial M_y^{(2)}}{\partial y} - K_s (w_2 - w_1) - \bar{m}_2 \frac{\partial^2 w_2}{\partial t^2} = P(x, y, t) \quad (2)$$

where $M_x^{(i)}, M_y^{(i)}$: moments per unit area applied by the core on the i-th layer middle surface in the x and y-direction, respectively, K_s : translational stiffness of the core per unit area, w_i : transverse displacement of the i-th layer, ($i=1,2$) and

$$\bar{m}_i = \rho_i h_i + \frac{1}{2} \rho_c h_c \ ,$$

where, ρ_i : density of the i-th layer, ($i=1,2$), h_i : thickness of the i-th layer, ρ_c : density of the core and h_c : thickness of the core.

Substituting for $m_x^{(i)}, m_y^{(i)}$ and $m_{xy}^{(i)}$ as known from the classical plate theory in equations (1) and (2) leads to the following governing equations of motion of the face layers:

$$D_1 \nabla^4 w_1 - \frac{\partial M_x^{(1)}}{\partial x} - \frac{\partial M_y^{(1)}}{\partial y} - K_s (w_2 - w_1) + \bar{m}_1 \frac{\partial^2 w_1}{\partial t^2} = 0 \quad (3)$$

$$D_2 \nabla^4 w_2 - \frac{\partial M_x^{(2)}}{\partial x} - \frac{\partial M_y^{(2)}}{\partial y} + K_s (w_2 - w_1) + \bar{m}_2 \frac{\partial^2 w_2}{\partial t^2} = P(x, y, t) \quad (4)$$

where D_1, D_2 are flexural rigidities of the lower and upper layers, respectively.

First Model

It will be shown in a later section, (STIFFNESS

PARAMETERS) that the moments applied by the core on the face layers could be written as in equations (30) and (31), and after substitution into equations (3) and (4), the governing equations of motion become:

$$D_1 \nabla^4 w_1 - K_r (\nabla^2 w_1 + \nabla^2 w_2) - K_s (w_2 - w_1) + \bar{m}_1 \frac{\partial^2 w_1}{\partial t^2} = 0 \quad (5)$$

$$D_2 \nabla^4 w_2 - K_r (\nabla^2 w_1 + \nabla^2 w_2) + K_s (w_2 - w_1) + \bar{m}_2 \frac{\partial^2 w_2}{\partial t^2} = P(x, y, t) \quad (6)$$

Second Model

Considering the infinitesimal elements in the upper and lower layers shown in Fig. (3a) and (3b) and taking the summation of forces in the x and y-directions yield the following equations:

$$\frac{\partial N_x^{(1)}}{\partial x} + \frac{\partial N_{yx}^{(1)}}{\partial y} - Q_x^{(1)} = 0 \quad (7)$$

$$\frac{\partial N_y^{(1)}}{\partial y} + \frac{\partial N_{xy}^{(1)}}{\partial x} - Q_y^{(1)} = 0 \quad (8)$$

$$\frac{\partial N_x^{(2)}}{\partial x} + \frac{\partial N_{yx}^{(2)}}{\partial y} + Q_x^{(2)} = 0 \quad (9)$$

$$\frac{\partial N_y^{(2)}}{\partial y} + \frac{\partial N_{xy}^{(2)}}{\partial x} + Q_y^{(2)} = 0 \quad (10)$$

where $Q_x^{(i)}, Q_y^{(i)}$ are the forces per unit area applied by the core on the i-th layer in the x and y-direction, respectively. These forces are given in terms of in plane and transverse displacements, as derived in the stiffness parameters section.

Substituting $N_x^{(i)}, N_y^{(i)}, N_{xy}^{(i)}, Q_x^{(i)}$ and $Q_y^{(i)}$ into equations (7), (8), (9), (10), (4) and (5) yields the following equations (11) through (16), respectively:

$$A_1 \left[\frac{\partial^2 u_1^o}{\partial x^2} + \frac{1-\nu_1}{2} \frac{\partial^2 u_1^o}{\partial y^2} + \frac{1+\nu_1}{2} \frac{\partial^2 v_1^o}{\partial x \partial y} \right] - G_c \left[\frac{h_2}{2h_c} \frac{\partial w_2}{\partial x} + \left(\frac{h_1}{2h_c} + 1 \right) \frac{\partial w_1}{\partial x} - \Phi_x \right] = 0 \quad (11)$$

$$A_1 \left[\frac{\partial^2 v_1^o}{\partial y^2} + \frac{1-\nu_1}{2} \frac{\partial^2 v_1^o}{\partial x^2} + \frac{1+\nu_1}{2} \frac{\partial^2 u_1^o}{\partial x \partial y} \right] - G_c \left[\frac{h_2}{2h_c} \frac{\partial w_2}{\partial y} + \left(\frac{h_1}{2h_c} + 1 \right) \frac{\partial w_1}{\partial y} - \Phi_y \right] = 0 \quad (12)$$

$$D_1 \nabla^4 w_1 - K_{11} \nabla^2 w_1 - K_{21} \nabla^2 w_2 + K_1 \left(\frac{\partial \Phi_x}{\partial x} + \frac{\partial \Phi_y}{\partial y} \right) - K_s (w_2 - w_1) + \bar{m}_1 \frac{\partial^2 w_1}{\partial t^2} = 0 \quad (13)$$

$$A_2 \left[\frac{\partial^2 u_2^o}{\partial x^2} + \frac{1-\nu_2}{2} \frac{\partial^2 u_2^o}{\partial y^2} + \frac{1+\nu_2}{2} \frac{\partial^2 v_2^o}{\partial x \partial y} \right] + G_c \left[\left(\frac{h_2}{2h_c} + 1 \right) \frac{\partial w_2}{\partial x} + \frac{h_1}{2h_c} \frac{\partial w_1}{\partial x} - \Phi_x \right] = 0 \quad (14)$$

$$A_2 \left[\frac{\partial^2 v_2^o}{\partial y^2} + \frac{1-\nu_2}{2} \frac{\partial^2 v_2^o}{\partial x^2} + \frac{1+\nu_2}{2} \frac{\partial^2 u_2^o}{\partial x \partial y} \right] + G_c \left[\left(\frac{h_2}{2h_c} + 1 \right) \frac{\partial w_2}{\partial y} + \frac{h_1}{2h_c} \frac{\partial w_1}{\partial y} - \Phi_y \right] = 0 \quad (15)$$

$$D_2 \nabla^4 w_2 - K_{12} \nabla^2 w_1 - K_{22} \nabla^2 w_2 + K_2 \left(\frac{\partial \Phi_x}{\partial x} + \frac{\partial \Phi_y}{\partial y} \right) + K_s (w_2 - w_1) + \bar{m}_2 \frac{\partial^2 w_2}{\partial t^2} = P(x, y, t) \quad (16)$$

where u_i^o, v_i^o : are the membrane displacements of the middle surface at the i-th layer in the x and y-directions, respectively, ν_i Poissons ratio of the i-th

layer and $A = \frac{E_i h_i}{1 - \nu_i^2}$. Differentiate equation (11) with

$$A_1 \left[\frac{\partial^3 u_1^o}{\partial x^3} + \frac{\partial^3 u_1^o}{\partial x \partial y^2} + \frac{\partial^3 v_1^o}{\partial x^2 \partial y} + \frac{\partial^3 v_1^o}{\partial y^3} \right] - G_c \left[\frac{h_2}{2h_c} \nabla^2 w_2 + \left(\frac{h_1}{2h_c} + 1 \right) \nabla^2 w_1 - \left(\frac{\partial \Phi_x}{\partial x} + \frac{\partial \Phi_y}{\partial y} \right) \right] = 0 \quad (17)$$

$$A_2 \left[\frac{\partial^3 u_2^o}{\partial x^3} + \frac{\partial^3 u_2^o}{\partial x \partial y^2} + \frac{\partial^3 v_2^o}{\partial x^2 \partial y} + \frac{\partial^3 v_2^o}{\partial y^3} \right] + G_c \left[\left(\frac{h_2}{2h_c} + 1 \right) \nabla^2 w_2 + \frac{h_1}{2h_c} \nabla^2 w_1 - \left(\frac{\partial \Phi_x}{\partial x} + \frac{\partial \Phi_y}{\partial y} \right) \right] = 0 \quad (18)$$

Divide equation (17) by $(A_1 h_c)$ and equation (18) by $(A_2 h_c)$, then subtract equation (18) from (17) to get:

$$(\nabla^2 - \bar{A}) \left(\frac{\partial \Phi_x}{\partial x} + \frac{\partial \Phi_y}{\partial y} \right) + \frac{G_c}{h_c} \left(\frac{h_2 + 2h_c}{2h_c A_2} + \frac{h_2}{2h_c A_1} \right) \nabla^2 w_2 + \frac{G_c}{h_c} \left(\frac{h_1}{2h_c A_2} + \frac{h_1 + 2h_c}{2h_c A_1} \right) \nabla^2 w_1 = 0 \quad (19)$$

where: $\bar{A} = \frac{G_c}{h_c} \left(\frac{A_1 + A_2}{A_1 A_2} \right)$.

Substituting equation (19) into equations (13) and

respect to (x) and equation (12) with respect to (y) and add, then differentiate equation (14) with respect to (x) and equation (15) with respect to (y) and add, to get:

(16) leads to the following governing equations of motion of the face layers according to the second model:

$$D_1 \nabla^6 w_1 - C_1 \nabla^4 w_1 - K_{21} \nabla^4 w_2 + C_2 \nabla^2 w_1 + C_3 \nabla^2 w_2 + \bar{A} K_s (w_2 - w_1) + \bar{m}_1 \nabla^2 \ddot{w}_1 - \bar{A} \bar{m}_1 \ddot{w}_1 = 0 \quad (20)$$

$$D_2 \nabla^6 w_2 - C_4 \nabla^4 w_2 - K_{12} \nabla^4 w_1 + C_5 \nabla^2 w_2 + C_6 \nabla^2 w_1 - \bar{A} K_s (w_2 - w_1) + \bar{m}_2 \nabla^2 \ddot{w}_2 - \bar{A} \bar{m}_2 \ddot{w}_2 = \nabla^2 P - \bar{A} P \quad (21)$$

where: $C_1 = K_{11} + \bar{A} D_1$,

$$C_2 = \bar{A} K_{11} - \frac{G_c K_1}{h_c} \left(\frac{h_1}{2h_c A_2} + \frac{h_1 + 2h_c}{2h_c A_1} \right) + K_s,$$

$$C_3 = \bar{A} K_{21} - \frac{G_c K_1}{h_c} \left(\frac{h_2 + 2h_c}{2h_c A_2} + \frac{h_2}{2h_c A_1} \right) - K_s,$$

$$C_4 = K_{22} + \bar{A} D_2,$$

$$C_5 = \bar{A} K_{22} - \frac{G_c K_2}{h_c} \left(\frac{h_2 + 2h_c}{2h_c A_2} + \frac{h_2}{2h_c A_1} \right) + K_s,$$

$$C_6 = \bar{A} K_{12} - \frac{G_c K_2}{h_c} \left(\frac{h_1}{2h_c A_2} + \frac{h_1 + 2h_c}{2h_c A_1} \right) - K_s.$$

STIFFNESS PARAMETERS

The extensional stiffness per unit area of the core with thickness h_c for both models is simply:

$$K_s = \frac{E_c}{h_c}. \quad (22)$$

The stiffness parameters of equivalent rotational springs for the two different models are derived in the following sections.

First Model

The transverse displacement of the soft visco-elastic core is defined by the transverse displacements of the

lower and upper layers and varies linearly. Also, according to the assumption that there is a perfect bond between the layers and the core at the interfaces, the in-plane displacements in the core are determined using the in-plane displacements of the lower and upper layers at the interfaces and assuming linear variations. The in-plane displacements in the lower and upper layers are defined according to the classical plate theory (for $i=1,2$) as follows:

$$u_i(x, y, z_i, t) = -z_i \frac{\partial w_i}{\partial x} \quad (23)$$

$$v_i(x, y, z_i, t) = -z_i \frac{\partial w_i}{\partial y} \quad (24)$$

The transverse and in-plane displacements in the core are as follows:

$$w_c = \left(\frac{w_1 - w_2}{h_c}\right)z_c + \frac{Z_o - h_1}{h_c}w_2 + \frac{h_c + h_1 - Z_o}{h_c}w_1 \quad (25)$$

$$u_c(x, y, z_c, t) = \left(\frac{u_1 \Big|_{(x,y,-\frac{h_1}{2},t)} - u_2 \Big|_{(x,y,\frac{h_2}{2},t)}}{h_c}\right)z_c + \frac{Z_o - h_1}{h_c}u_2 \Big|_{(x,y,\frac{h_2}{2},t)} + \frac{h_1 + h_c - Z_o}{h_c}u_1 \Big|_{(x,y,-\frac{h_1}{2},t)} \quad (26)$$

$$v_c(x, y, z_c, t) = \left(\frac{v_1 \Big|_{(x,y,-\frac{h_1}{2},t)} - v_2 \Big|_{(x,y,\frac{h_2}{2},t)}}{h_c}\right)z_c + \frac{Z_o - h_1}{h_c}v_2 \Big|_{(x,y,\frac{h_2}{2},t)} + \frac{h_1 + h_c - Z_o}{h_c}v_1 \Big|_{(x,y,-\frac{h_1}{2},t)} \quad (27)$$

$$\text{where: } Z_o = \frac{E_2 h_2 \left(\frac{h_2}{2} + h_c + h_1\right) + E_c h_c \left(\frac{h_c}{2} + h_1\right) + E_1 \frac{h_1^2}{2}}{E_2 h_2 + E_c h_c + E_1 h_1}$$

Considering the element shown in Figure (4) in the xz -plane with unit length in the x -direction, the shear strain is defined as follows:

$$\gamma_{xz} = \frac{\partial u_c}{\partial z_c} + \frac{\partial w_c}{\partial x} \quad (28)$$

$$\gamma_{xz} = \left(\frac{h_2}{2h_c} - \frac{Z_c}{h_c} + \frac{Z_o - h_1}{h_c}\right)\frac{\partial w_2}{\partial x} + \left(\frac{h_1}{2h_c} + \frac{Z_c}{h_c} + \frac{h_1 + h_c - Z_o}{h_c}\right)\frac{\partial w_1}{\partial x} \quad (29)$$

Consider the element shown in Fig. (4), define $M_x^{(1)}$ and $M_x^{(2)}$ to be the total applied moment from the core on the lower and upper layers middle surface, respectively as follows:

$$M_x^{(i)} = \frac{dM_x}{2} = \frac{Q_x}{2}$$

Substituting equations (25) and (26) into equation (28) yields the following shear strain in terms of upper and lower layers transverse displacements:

Recall that $\tau_{xz} = G_c \gamma_{xz}$ and $Q_x = \int_{(Z_o - h_1 - h_c)}^{(Z_o - h_1)} \tau_{xz} dz$, then $M_x^{(i)}$ can be written in the form:

$$M_x^{(i)} = K_r \left(\frac{\partial w_2}{\partial x} + \frac{\partial w_1}{\partial x}\right) \quad (30)$$

where:

$$K_r = \frac{A_1 K_{r1} + A_2 K_{r2}}{A_1 + A_2} \text{ and}$$

$$K_{r1} = \frac{G_c}{2} \left(\frac{h_1}{2} + h_1 + h_c - Z_o - \frac{(Z_o - h_1 + h_c)^2 - (Z_o - h_1)^2}{2h_c} \right)$$

$$K_{r2} = \frac{G_c}{2} \left(\frac{h_2}{2} + Z_o - h_1 + \frac{(Z_o - h_1 + h_c)^2 - (Z_o - h_1)^2}{2h_c} \right)$$

$$A_i = \frac{E_i h_i}{1 - \nu_i^2}, \quad i=1,2.$$

Similarly:

$$M_y^{(i)} = K_r \left(\frac{\partial w_2}{\partial y} + \frac{\partial w_1}{\partial y} \right) \quad (31)$$

$$\gamma_{xz} = \left(\frac{h_2}{2h_c} - \frac{z_c}{h_c} + \frac{Z_o - h_1}{h_c} \right) \frac{\partial w_2}{\partial x} + \left(\frac{h_1}{2h_c} + \frac{z_c}{h_c} + \frac{h_1 + h_c - Z_o}{2} \right) \frac{\partial w_1}{\partial x} - \Phi_x \quad (33)$$

where: $\Phi_x = \frac{u_1^o - u_2^o}{h_c}$.

Recall that $\tau_{xz} = G_c \gamma_{xz}$, $Q_x = \int_{(Z_o - h_1 - h_c)}^{(Z_o - h_1)} \tau_{xz} dz$, then the resultant shear stress can be defined as follows:

$$Q_x^{(1)} = G_c \left[\left(\frac{h_2}{2h_c} \right) \frac{\partial w_2}{\partial x} + \left(\frac{h_1}{2h_c} + 1 \right) \frac{\partial w_1}{\partial x} - \Phi_x \right] \quad (34)$$

$$Q_x^{(2)} = G_c \left[\left(\frac{h_2}{2h_c} + 1 \right) \frac{\partial w_2}{\partial x} + \left(\frac{h_1}{2h_c} \right) \frac{\partial w_1}{\partial x} - \Phi_x \right] \quad (35)$$

Consider the element shown in Fig. (6), define $M_x^{(1)}$ and $M_x^{(2)}$ to be the total applied moment from the core on the lower and upper layers middle surface, respectively as follows:

$$M_x^{(1)} = M_x + Q_x^{(1)} \frac{h_1}{2} \quad (36)$$

$$K_{11} = G_c \left[\frac{3h_1}{4} + \frac{h_1^2}{4h_c} + \frac{h_1 + h_c - Z_o}{2} - \frac{(h_1 + h_c - Z_o)^2 - (Z_o - h_1)^2}{4h_c} \right],$$

Second Model

In the second model, the membrane displacements at the middle surfaces of face layers were included. The displacements of the sandwich plate are as shown in Fig. (5), where the transverse displacement in the core, which varies linearly, is completely determined by the transverse displacements of the face layers as defined in equation (25).

The shear strain can be defined as follows:

$$\gamma_{xz} = \frac{u_1 \Big|_{(x,y,-\frac{h_1}{2},t)} - u_2 \Big|_{(x,y,\frac{h_2}{2},t)}}{h_c} + \frac{\partial w_c}{\partial x} - \frac{u_1^o - u_2^o}{h_c} \quad (32)$$

Substituting equations (23) and (25) into equation (32) leads to:

$$M_x^{(2)} = M_x + Q_x^{(2)} \frac{h_2}{2} \quad (37)$$

where: $M_x = \frac{dM_x}{2} = \frac{Q_x}{2}$.

Substituting equations (34), (35) and the value of M_x into equations (36) and (37) leads to:

$$M_x^{(1)} = K_{21} \frac{\partial w_2}{\partial x} + K_{11} \frac{\partial w_1}{\partial x} - K_1 \Phi_x \quad (38)$$

$$M_x^{(2)} = K_{22} \frac{\partial w_2}{\partial x} + K_{12} \frac{\partial w_1}{\partial x} - K_2 \Phi_x \quad (39)$$

Similarly, $M_y^{(1)}$ and $M_y^{(2)}$ are obtained as follows:

$$M_y^{(1)} = K_{21} \frac{\partial w_2}{\partial y} + K_{11} \frac{\partial w_1}{\partial y} - K_1 \Phi_y \quad (40)$$

$$M_y^{(2)} = K_{22} \frac{\partial w_2}{\partial y} + K_{12} \frac{\partial w_1}{\partial y} - K_2 \Phi_y \quad (41)$$

where

$$K_{12} = G_c \left[\frac{h_1}{4} + \frac{h_1 h_2}{4h_c} + \frac{h_1 + h_c - Z_o}{2} - \frac{(h_1 + h_c - Z_o)^2 - (Z_o - h_1)^2}{4h_c} \right],$$

$$K_{21} = G_c \left[\frac{h_2}{4} + \frac{h_1 h_2}{4h_c} + \frac{Z_o - h_1}{2} + \frac{(h_1 + h_c - Z_o)^2 - (Z_o - h_1)^2}{4h_c} \right],$$

$$K_{22} = G_c \left[\frac{3h_2}{4} + \frac{h_2^2}{4h_c} + \frac{Z_o - h_1}{2} - \frac{(h_1 + h_c - Z_o)^2 - (Z_o - h_1)^2}{4h_c} \right],$$

$$K_1 = \frac{G_c}{2} (h_1 + h_c),$$

$$K_2 = \frac{G_c}{2} (h_2 + h_c).$$

METHOD OF SOLUTION

The modal superposition method is used to solve the governing equations of motion. For free vibration of undamped sandwich plates, we seek solutions of the governing equations in the form:

$$w_1 = \sum_{m=1}^{\infty} \sum_{n=1}^{\infty} (A_{mn})_1 \phi_{mn} e^{i\omega t} \tag{42}$$

$$w_2 = \sum_{m=1}^{\infty} \sum_{n=1}^{\infty} (A_{mn})_2 \phi_{mn} e^{i\omega t} \tag{43}$$

$$w_1(x, y, t) = \sum_{m=1}^{\infty} \sum_{n=1}^{\infty} \phi_{mn} [(A_{mn})_{11} (Z_{mn})_1 + (A_{mn})_{12} (Z_{mn})_2] \tag{45}$$

$$w_2(x, y, t) = \sum_{m=1}^{\infty} \sum_{n=1}^{\infty} \phi_{mn} [(A_{mn})_{21} (Z_{mn})_1 + (A_{mn})_{22} (Z_{mn})_2] \tag{46}$$

$$\begin{aligned} & \sum_{m=1}^{\infty} \sum_{n=1}^{\infty} \bar{m}_1 \phi_{mn} (A_{mn})_{11} (\ddot{Z}_{mn})_1 + [D_1 \nabla^4 \phi_{mn} (A_{mn})_{11} - K_s \phi_{mn} ((A_{mn})_{21} - (A_{mn})_{11}) - \\ & K_r \nabla^2 \phi_{mn} ((A_{mn})_{11} + (A_{mn})_{21})] (Z_{mn})_1 + \bar{m}_1 \phi_{mn} (A_{mn})_{12} (\ddot{Z}_{mn})_2 + [D_1 \nabla^4 \phi_{mn} (A_{mn})_{12} - \\ & K_s \phi_{mn} ((A_{mn})_{22} - (A_{mn})_{12}) - K_r \nabla^2 \phi_{mn} ((A_{mn})_{22} + (A_{mn})_{12})] (Z_{mn})_2 \} = 0 \end{aligned} \tag{47}$$

where: $(A_{mn})_1$ and $(A_{mn})_2$ are the amplitudes of response of the lower and upper plates, respectively, and ϕ_{mn} represents the different modes of vibrations. Substituting equations (42) and (43) in the governing equations for the case $P(x,y,t)=0.0$ and solving the eigen-value problem lead to the determination of the natural frequencies of the sandwich plate. For simply supported boundary conditions, the modal shape functions could be written in the following form:

$$\phi_{mn} = \sin\left(\frac{m\pi}{a} x\right) \sin\left(\frac{n\pi}{b} y\right) \tag{44}$$

First Model Solution

The solution of equations (5) and (6) is assumed to be in the form:

$$\sum_{m=1}^{\infty} \sum_{n=1}^{\infty} \{ \bar{m}_2 \phi_{mn}(A_{mn})_{21} (\ddot{Z}_{mn})_1 + [D_2 \nabla^4 \phi_{mn}(A_{mn})_{21} + K_s \phi_{mn}((A_{mn})_{21} - (A_{mn})_{11}) - K_r \nabla^2 \phi_{mn}((A_{mn})_{21} + (A_{mn})_{11})] (Z_{mn})_1 + \bar{m}_2 \phi_{mn}(A_{mn})_{22} (\ddot{Z}_{mn})_2 + [D_2 \phi_{mn}(A_{mn})_{22} + K_s \phi_{mn}((A_{mn})_{22} - (A_{mn})_{12}) - K_r \nabla^2 \phi_{mn}((A_{mn})_{22} + (A_{mn})_{12})] (Z_{mn})_2 \} = P(x, y, t) \quad (48)$$

Substituting equations (42), (43) and (44) into equations (5) and (6), introducing the first natural frequency $(\omega_{mn})_1$, also introducing another sub-index in $(A_{mn})_1$ and $(A_{mn})_2$ to account for the first natural frequency, introducing the second natural frequency

$(\omega_{mn})_2$, and also introducing another sub-index in $(A_{mn})_1$ and $(A_{mn})_2$ to account for the second natural frequency. Using these four equations to simplify equations (47) and (48) leads to:

$$\sum_{m=0}^{\infty} \sum_{n=0}^{\infty} \{ \bar{m}_1 \phi_{mn}(A_{mn})_{11} (\ddot{Z}_{mn})_1 + \bar{m}_1 \phi_{mn}(\omega_{mn})_1^2 (A_{mn})_{11} (Z_{mn})_1 + \bar{m}_1 \phi_{mn}(A_{mn})_{11} (\ddot{Z}_{mn})_1 + \bar{m}_1 \phi_{mn}(\omega_{mn})_1^2 (A_{mn})_{11} (Z_{mn})_1 + \bar{m}_1 \phi_{mn}(A_{mn})_{12} (\ddot{Z}_{mn})_2 + \bar{m}_1 \phi_{mn}(\omega_{mn})_2^2 (A_{mn})_{12} (Z_{mn})_2 \} = 0 \quad (49)$$

$$\sum_{m=1}^{\infty} \sum_{n=1}^{\infty} \{ \bar{m}_2 \phi_{mn}(A_{mn})_{21} (\ddot{Z}_{mn})_1 + \bar{m}_2 \phi_{mn}(\omega_{mn})_1^2 (A_{mn})_{21} (Z_{mn})_1 + \bar{m}_2 \phi_{mn}(A_{mn})_{22} (\ddot{Z}_{mn})_2 + \bar{m}_2 \phi_{mn}(\omega_{mn})_2^2 (A_{mn})_{22} (Z_{mn})_2 \} = P(x, y, t) \quad (50)$$

The orthogonality condition between the normal amplitudes could be written in the following form:

$$\sum_{k=1}^2 \bar{m}_k (A_{mn})_{ki} (A_{mn})_{kj} = 0 \quad , i \neq j ; \quad (51)$$

where $i=1,2$ and $j=1,2$.

Multiplying equation (49) by $(A_{mn})_{11}$ and equation (50) by $(A_{mn})_{21}$, then adding the two equations, then

multiplying equation (62) by $(A_{mn})_{12}$ and equation (50) by $(A_{mn})_{22}$, then adding the two equations, and using equation (51) lead to:

$$\sum_{m=1}^{\infty} \sum_{n=1}^{\infty} (\bar{m}_1 (A_{mn})_{11}^2 + \bar{m}_2 (A_{mn})_{21}^2) \phi_{mn} (\ddot{Z}_{mn})_1 + (\bar{m}_1 (A_{mn})_{11}^2 + \bar{m}_2 (A_{mn})_{21}^2) (\omega_{mn})_1^2 \phi_{mn} (Z_{mn})_1 = (A_{mn})_{21} P(x, y, t) \quad (52)$$

$$\sum_{m=1}^{\infty} \sum_{n=1}^{\infty} (\bar{m}_1 (A_{mn})_{12}^2 + \bar{m}_2 (A_{mn})_{22}^2) \phi_{mn} (\ddot{Z}_{mn})_2 + (\bar{m}_1 (A_{mn})_{12}^2 + \bar{m}_2 (A_{mn})_{22}^2) (\omega_{mn})_2^2 \phi_{mn} (Z_{mn})_2 = (A_{mn})_{22} P(x, y, t) \quad (53)$$

The orthogonality condition between the normal modes could be written in the following form:

$$\int_0^a \int_0^b \bar{m}_i \phi_{mn} \phi_{gj} dx dy = 0, \text{ for } m, n \neq g, j \quad (54)$$

Consider equation (52) and (53), multiply both of them by ϕ_{gj} and integrate over the area of the sandwich plate, then simplify the resulting equations by equation (54) to obtain:

$$(\ddot{Z}_{mn})_1 + (\omega_{mn})_1^2 (Z_{mn})_1 = (F_{mn})_{21} \quad (55)$$

$$(\ddot{Z}_{mn})_2 + (\omega_{mn})_2^2 (Z_{mn})_2 = (F_{mn})_{22} \quad (56)$$

where for $i=1,2; j=1,2$:

$$(M_{mn})_{ij} = \int_0^a \int_0^b (A_{mn})_{ij}^2 \bar{m}_i \phi_{mn}^2 dx dy,$$

$$(F_{mn})_{21} = \frac{\int_0^a \int_0^b (A_{mn})_{21} P(x, y, t) \phi_{mn} dx dy}{(M_{mn})_{11} + (M_{mn})_{21}},$$

$$(F_{mn})_{22} = \frac{\int_0^a \int_0^b (A_{mn})_{22} P(x, y, t) \phi_{mn} dx dy}{(M_{mn})_{12} + (M_{mn})_{22}}.$$

Second Model Solution

Following the same previous procedure to solve the governing equations of motion of the second model; i.e equations (20) and (21) will lead to the same previous equations with new definitions as follows:

where for $i=1,2 ; j=1,2$:

$$(M_{mn})_{ij} = \int_0^a \int_0^b \bar{m}_i (A_{mn})_{ij}^2 \phi_{mn} (\nabla^2 \phi_{mn} - \bar{A} \phi_{mn}) dx dy,$$

$$(F_{mn})_{21} = \frac{\int_0^a \int_0^b (A_{mn})_{21} \phi_{mn} (\nabla^2 P - \bar{A} P) dx dy}{(M_{mn})_{11} + (M_{mn})_{21}},$$

$$(F_{mn})_{22} = \frac{\int_0^a \int_0^b (A_{mn})_{22} \phi_{mn} (\nabla^2 P - \bar{A} P) dx dy}{(M_{mn})_{12} + (M_{mn})_{22}}.$$

IMPACT LOADS

For the forced vibration of sandwich plates, the following impact loads are considered:

Half Sine Impulse

The excitation applied to the sandwich plate is taken in the form of a half sine impulse as shown in Figure (7a). According to (Grover and Kapur, 1982), this loading could be represented as:

$$P(x, y, t) = \begin{cases} f(x, y) \sin(\omega t), & 0 \leq t \leq \tau \\ 0, & t \geq \tau \end{cases}$$

where according to the same reference the loading function $f(x, y)$ could be expressed as:

$$f(x, y) = \bar{m} v \omega g(x, y)$$

where: $\bar{m} = \bar{m}_1 + \bar{m}_2$, v : Projectile velocity, ω : Frequency of the impact loading, τ : Impact duration.

Step Impulse

For this type of impact loading, as shown in Figure (7b), it is assumed that the energy and duration of impact of the step loading are the same as for the half sine impulse, so it is easily proved that:

$$f_1 = \frac{2\bar{m}v\omega}{\pi}$$

where the loading function is written in the form:

$$P(x, y, t) = \begin{cases} f_1 g(x, y), & 0 \leq t \leq \tau \\ 0, & t \geq \tau \end{cases}$$

Triangular Impulse

Also, it is assumed that for this type of loading, as shown in Figure (8c), the energy and the impact

duration of the triangular pulse are the same as the half sine pulse, that is

$$f_2 = \frac{4\bar{m}v\varpi}{\pi}$$

where the loading function is written in the form:

$$P(x, y, t) = \begin{cases} f_2 g(x, y) \left(\frac{\tau - t}{\tau}\right), & 0 \leq t \leq \tau \\ 0, & t \geq \tau \end{cases}$$

Table 1: Geometry and material properties of sandwich plates

Property	Plate # 1	Plate # 2	Plate # 3
a & b (mm)	450	20	450
h ₁ & h ₂ (mm)	5	1	2.5
h _c (mm)	50	2	2.5
E ₁ & E ₂ (Gpa)	16.7	210	68.65
ν ₁ & ν ₂	0.3	0.3	0.34
ρ ₁ & ρ ₂ (kg/m ³)	1760	7800	2746
G _c (Gpa)	0.018	0.0021	0.01373
ν _c	0.32	0.45	0.45
ρ _c (kg/m ³)	48	780	1373

Table 2: Natural frequencies (Hz) for sandwich plate #1

Mode Number (m,n)	Present Study		Reference [5]	Reference [9]
	Model (1)	Model (2)		
(1,1)	356.1	354.5	340.2	358.79
(1,2)	578.2	574.76	553.7	593.55
(2,2)	750.0	731.82	719.76	771.51
(1,3)	852.14	819.71	818.89	876.21
(2,3)	994.4	935.63	957.4	1020.9
(3,3)	1213.54	1100.78	1171.62	1241.53

NUMERICAL RESULTS AND DISCUSSION

In this study, sandwich plates with various geometric configurations and material properties were considered. The geometry and material properties of the sandwich plates used are shown in Table (1). Table (2) shows natural frequencies of symmetrical sandwich plate # 1, where the first and second models were considered and compared with (Sayir and Koller, 1986; Lee and Kim, 1997). The results of the two models and those of (Sayir and Koller, 1986; Lee and Kim, 1997) are in good agreement for low modes, while for higher modes there is a little difference. The slight difference in the results of the two models and those of (Lee and Kim, 1997), in comparison to those of (Sayir and Koller, 1986), is attributed to that only the first term is considered in the asymptotic solution for the elasticity equations in (Lee and Kim, 1997). Figure 8 shows the variations of the non-dimensional natural frequency ($\omega a^2 \sqrt{(\bar{m}_1 + \bar{m}_2)/(D_1 + D_2)}$) with the non-dimensional core thickness (h_c/h_2) for different values of the second layer non-dimensional thickness (h_2/a). Sandwich plate #2 was considered and the lower four natural frequencies $\omega_{1,1}$, $\omega_{1,2}$, $\omega_{2,2}$, $\omega_{1,3}$ were computed. It can be seen from this Figure that the results of the present two models agree well with those of (Lee and Kim, 1997) for a thick core. The difference in the results obtained using the first model and those obtained in (Lee and Kim, 1997), for low core thickness ratio, and especially for higher modes, is due to the non-inclusion of the overall bending in the sandwich plate in the first model. Also, the in-plane displacements at the middle planes of the upper and lower layers were not considered in the formulation of the first model. Figure 9 depicts the time history of shock response of sandwich plate #3 due to a half sine impulse distributed over the whole plate area. Different values of the core shear modulus; 13.73, 68.68 and 343.25 MPa are used. Small difference is observed between model (2) and (Grover and Kapur, 1982) for

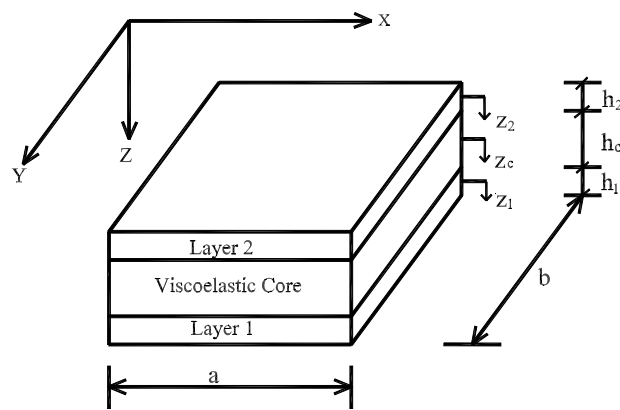


Figure 1: Geometry and Coordinates of Three Layered Sandwich Plate

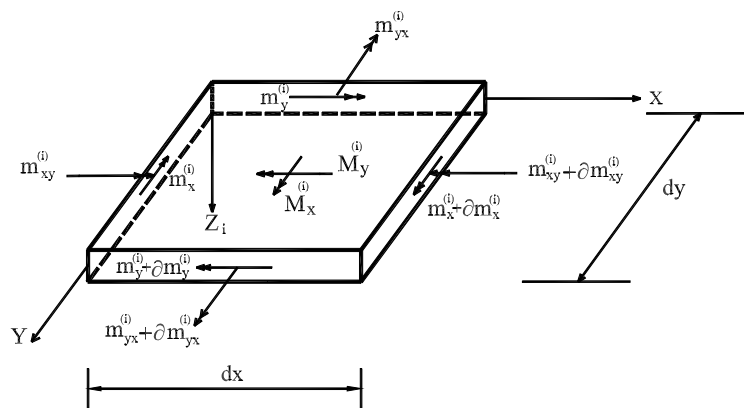
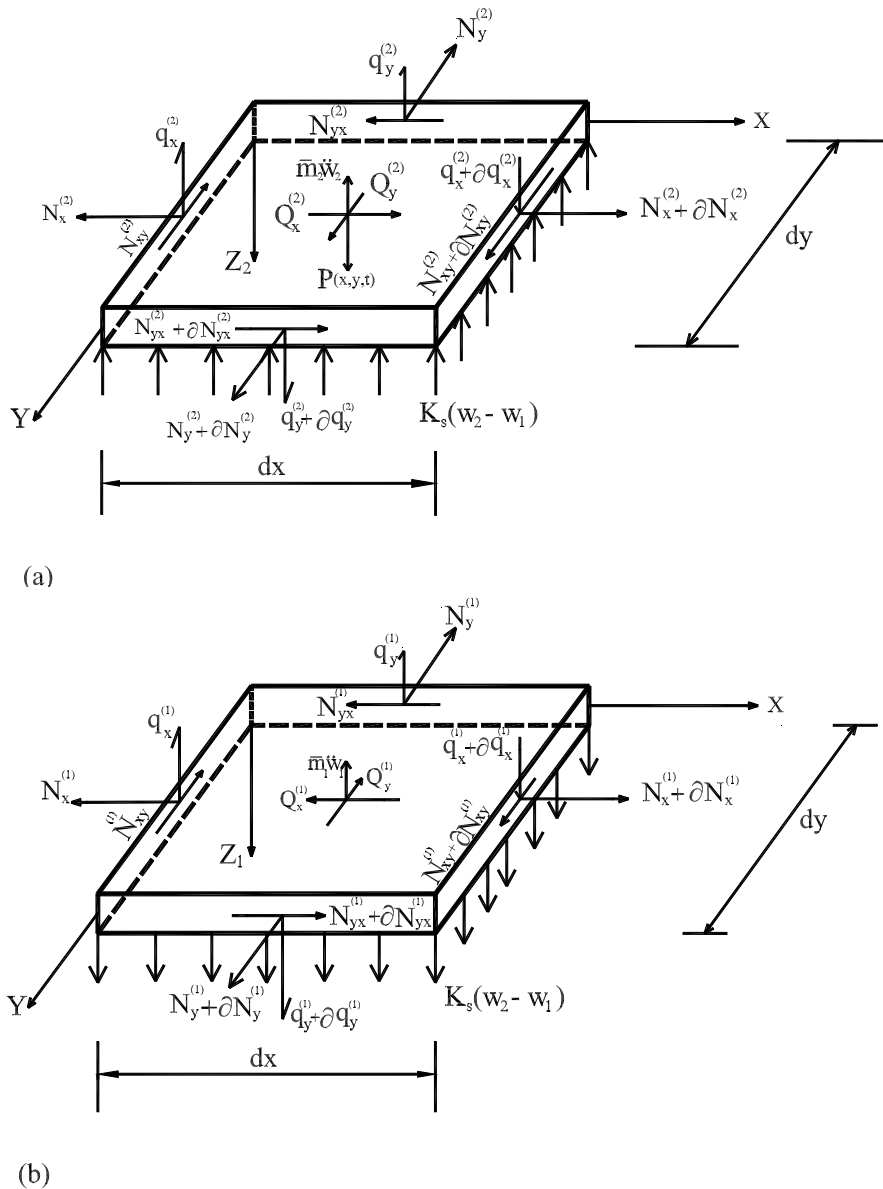


Figure 2: Infinitesimal Element in the i-th Layer Showing the Layer Moments

the values of amplitudes and periods of oscillation. This is due to the inclusion of damping properties of the core material in (Grover and Kapur, 1982) on one hand and the inclusion of deformability of the core (ϵ_c) in model (2) on the other hand. A large difference in the results obtained using model (1) is observed, especially for large shear modulus of the core. For a relatively strong core, the period of oscillation and the amplitude of response are not accurately determined using model (1). This can be attributed to the fact that the global bending of the plate and the local contribution of the core through normal stresses are not accounted for. Model (1) could be used for weak cores only. Fig. 9a shows

that the inclusion of damping properties of the core is more pronounced for a smaller value of shear modulus. The variation of peak response with G_c/E_1 ratio is investigated in Fig. (10), in which G_c/E_1 is varied over a wide range. Sandwich plate #3 was considered with ($a=b=300$ mm) and the other parameters are as given in Table (1). It is obvious that, as the core shear modulus ratio increases (in the range 0.0001-0.001), the peak response decreases rapidly. For values of G_c/E_1 greater than 0.001, the peak response doesn't change much. The results of the two models seem to have a very good agreement with those of (Grover and Kapur, 1982) for a semi-rigid core, while for a high shear modulus ratio of



**Figure 3: Infinitesimal Element in the Face Layers Showing the Face Layer Forces
(a) Upper Layer (b) Lower Layer**

the core, it is found that model (1) yields inaccurate results. The difference between the results of the two models and those of (Grover and Kapur, 1982) for very low core shear modulus is due to that the damping effect in the equations of motion of (Grover and Kapur, 1982) increases as the core shear modulus decreases. The variation of the peak response with h_c/h_1 ratio for

different values of ($G_c=343.25, 68.65$ and 13.73 MPa) is shown in Fig. (11). Sandwich plate #3 is used with variable h_c and G_c and all other parameters are as in Table (1). It is observed that, as the core thickness ratio increases, the peak response decreases due to that the plate stiffness increases through the increment in the shear parameters in the governing equations of motion.

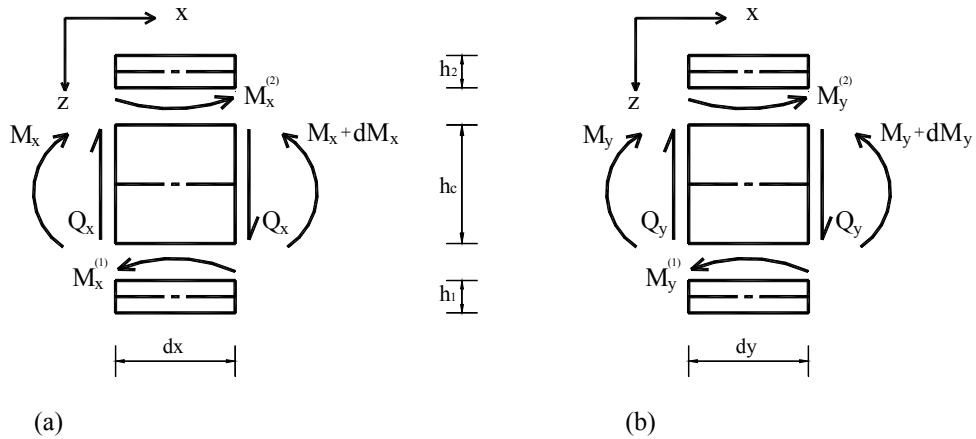


Figure 4: Infinitesimal Elements in the Sandwich Plate According to Model (1) Showing Shear Forces and Moments per Unit Length in the Core in (a) x-z Plane, (b) y-z Plane

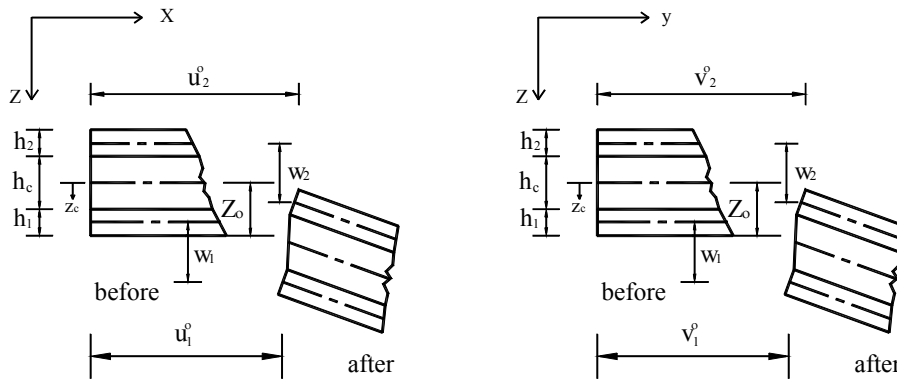


Figure 5: Displacements of Three Layered Sandwich Plate According to Model (2) in (a) x-z Plane, (b) y-z Plane

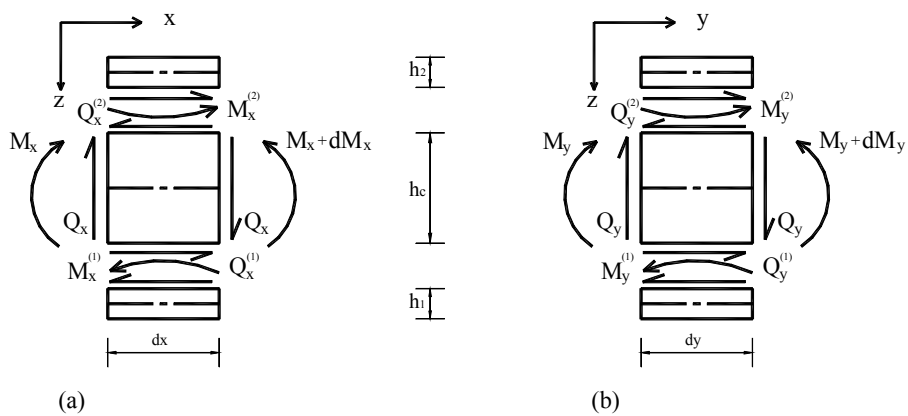


Figure 6: Infinitesimal Elements in the Sandwich Plate According to Model (2) Showing Interface Shear Forces and Moments per Unit Length in (a) x-z Plane, (b) y-z Plane

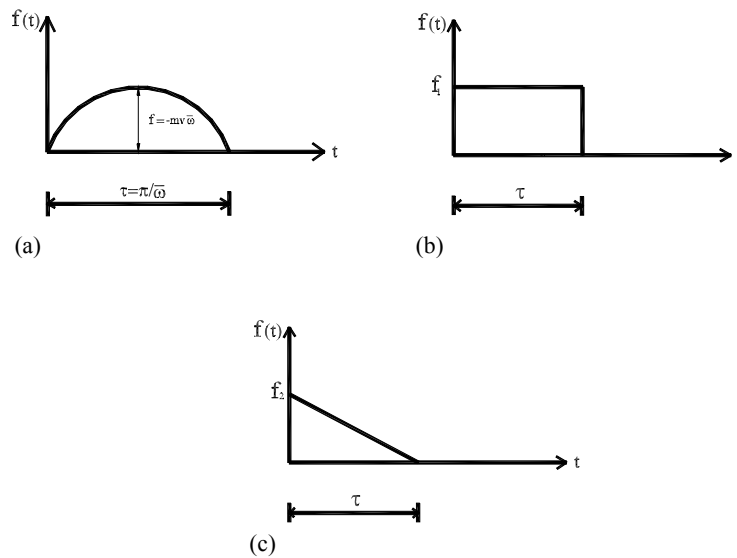


Figure 7: Different Types of Dynamic Loading (a) Half Sine Impulse, (b) Rectangular Impulse, (c) Triangular Impulse

The Figure shows that for a very low core thickness ratio there is a considerable difference in the results of model (1), while the results of model (2) and (Grover and Kapur, 1982) agree well. This may be due to that only the local bending of the face layers around their middle surface was considered in model (1). It is also obvious that, for a higher thickness ratio of the core the results of the two models and those of (Grover and Kapur, 1982) are almost the same. This is a good indication that the behavior of the sandwich plate at a higher core ratio is a local bending of the face plates and a transverse shear deformation of the core. Fig. (12) shows the transverse deflection pattern along the x-axis and at $y=b/2$ for a half sine impulsive concentric loading at the center of sandwich plate #1 at different times. Fig. (13) shows the face layers deflection pattern for the same previous loading in a three-dimensional plot. It can be noticed that there is a considerable difference in the deflections of the upper and lower layers at the region of concentrated impact load. This may be attributed to that the core is very thick compared to the face plates and also the core shear modulus is very low

which will cause the upper layer to bend locally following the deformed core and the core will distribute the concentrated load over a wider area on the lower layer. It is also observed that, away from the vicinity of concentrated load, the lower and upper layers have the same deflection. Fig. (14) shows the values of displacement of the upper and lower layers at the center of sandwich plate #1 due to half sine point loading at the center of the plate. The solid and dashed lines represent deformations of the upper and lower layers, respectively. It can be seen from this Figure that the two layers deflect differently during the impact duration (τ). After the contact duration, the two layers deflect in the same amount and the two curves merge into a single one as shown in the Figure. The dash-dot line represents the response of the two layers excluding the normal deformation in the core (ε_z), so the displacements of these two layers are the same, thus only one curve is shown. Fig. (15) shows the time-history of shock response due to different types of impact loading; half sine, step and triangular impulses. The different types of loading have the same energy and impact duration. It is

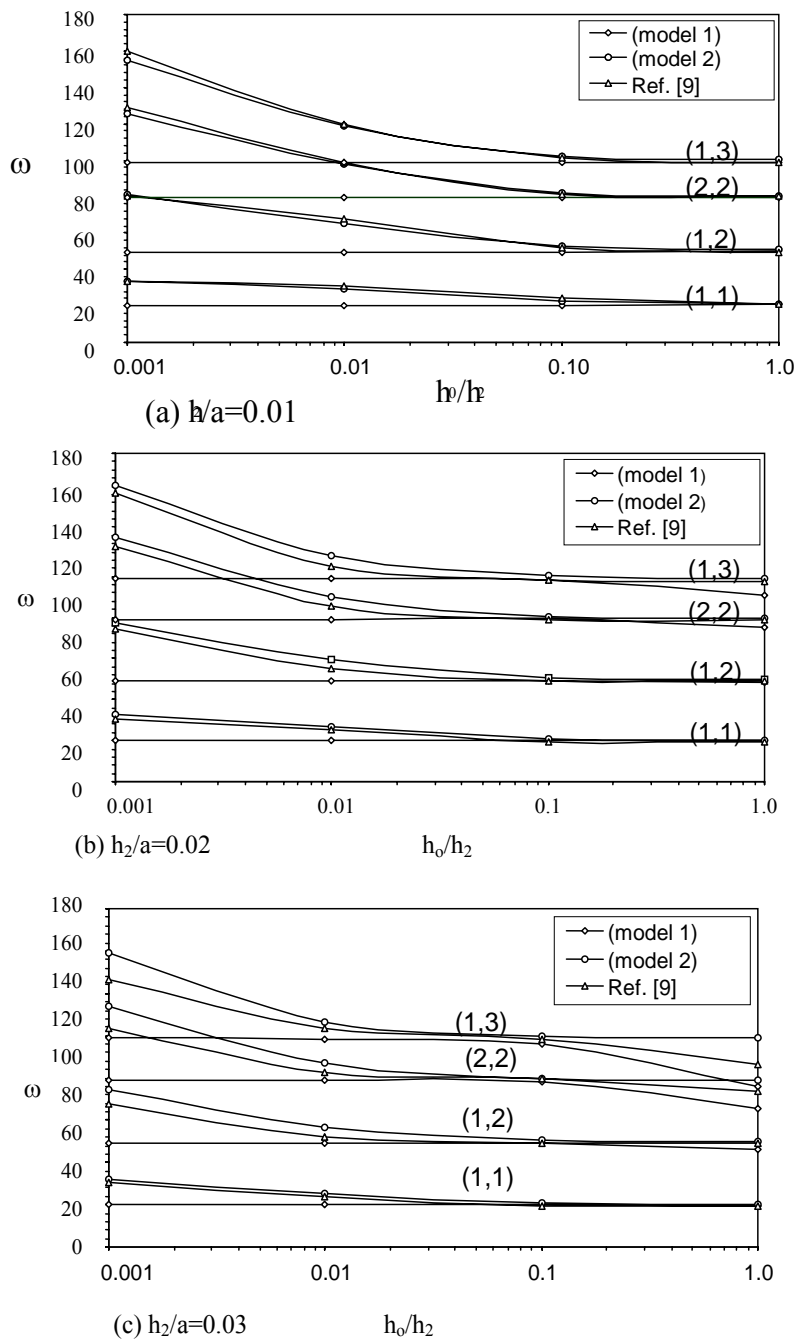


Figure 8: Variations of the Non-dimensional Natural Frequency(ω) with Core Thickness Ratio for Sandwich Plate #2 for $h_1/h_2 = 0.5$

Note: Ref. [9]= Lee and Kim (1997)

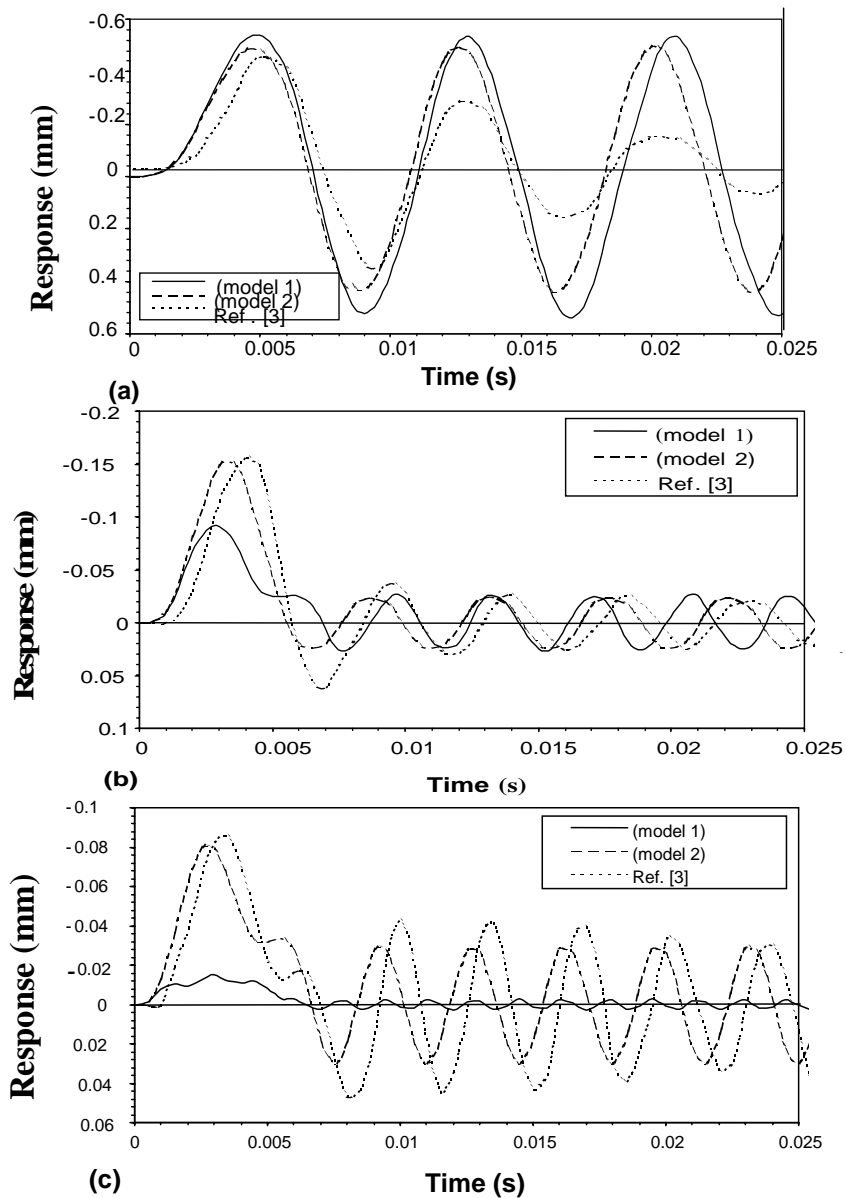


Figure 9: Time History of Shock Response of Sandwich Plate #3 (a) $G_c=13.73$ MPa, (b) $G_c=68.65$ MPa, (c) $G_c=343.25$ MPa

Note: Ref. [3]= Grover and Kapur (1982)

obvious that the triangular impulse has the largest peak compared to the half sine impulse and the step impulse during the impact duration. Also, it is obvious that the peak responses of the triangular and the step impulses occur at the same time and earlier than the half sine

impulse. It is noticed that after the impact duration, the response of the two layers due to the half sine impulse is the same, while for the other two types of loading there is a little difference.

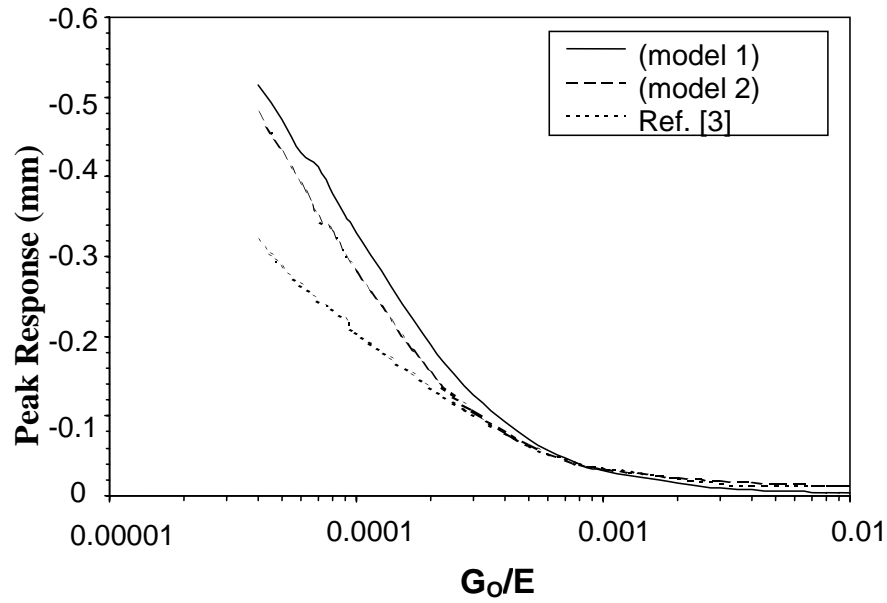


Figure 10: Variations of the Peak Response at the Center of Sandwich Plate #3 with Core Shear Modulus Ratio (G_0/E_1) Due to Half Sine Shock Pulse with $\varpi = 500$ rad/s

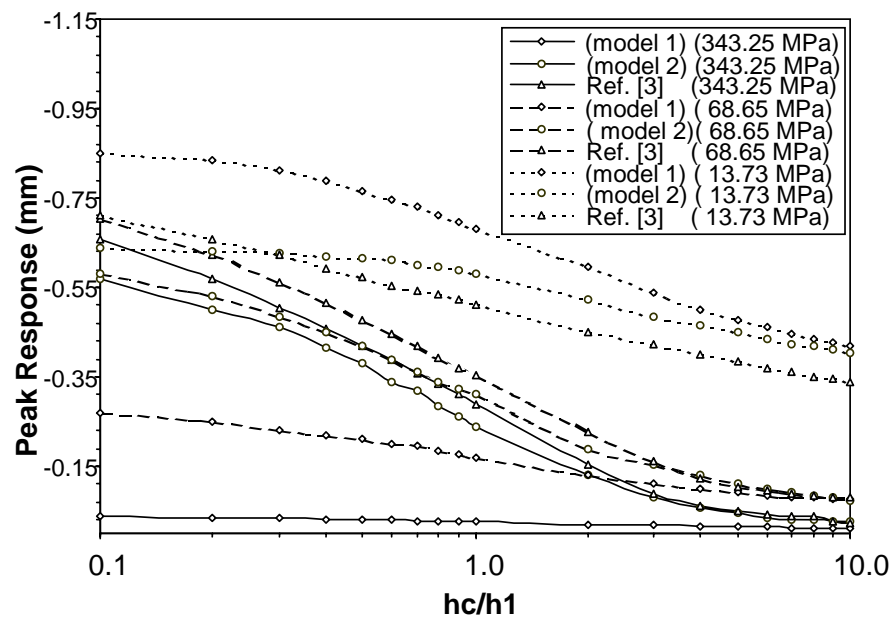


Figure 11: Peak Response at the Center of Sandwich Plate #3 versus Core Thickness Ratio (h_c/h_1) for Different Core Shear Modulus 343.25, 68.65 and 13.73 MPa

Note: Ref. [3]= Grover and Kapur (1982)

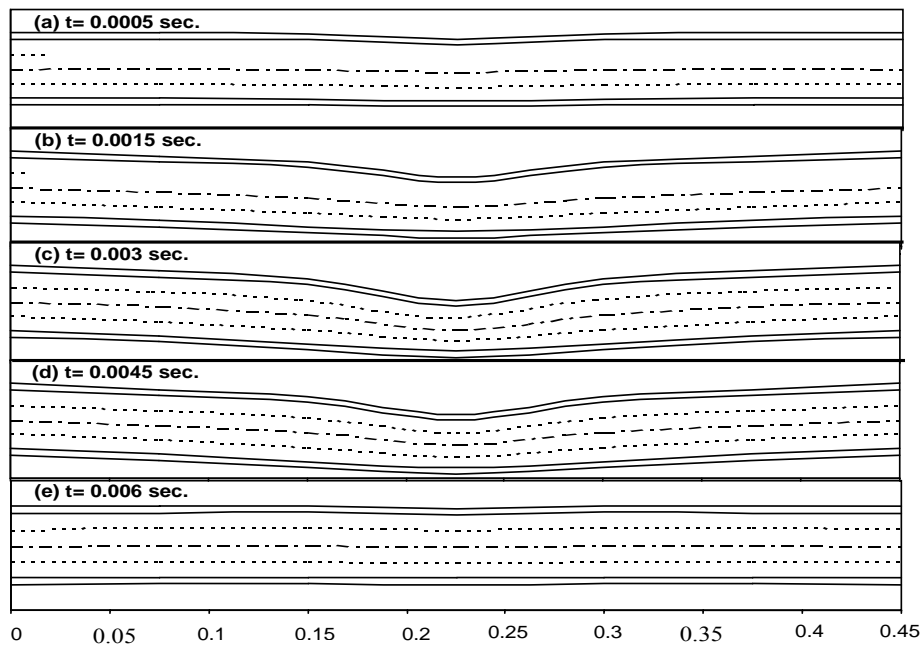


Figure 12: Transverse Deflection Pattern along the x-axis and $y=b/2$ for Sandwich Plate #1 Impacted by a Point Loading at the Center at (a) $t=0.0005$ sec., (b) $t=0.0015$ sec., (c) $t=0.003$ sec., (d) $t=0.0045$ sec., (e) $t=0.006$ sec

CONCLUSIONS

The response of simply supported three-layered sandwich plates subjected to impact loading has been investigated. The governing equations of motion for undamped sandwich plates could be solved in a closed form, following the modal superposition method. Based on the results discussed earlier, the following conclusions could be drawn: The first model works very well for sandwich plates with a thick and small shear modulus core. The in-plane displacements at the middle

surface of the face layers become more important for sandwich plates with a core having a large shear modulus or a core with a thickness less than the face layers thickness. The normal deformation in the core must be included in the sandwich plate model to account for the difference in displacements of the face layers, especially at the region of impact. After the impact duration, the two layers exhibit the same response and the core normal deformation has no effect on the response.

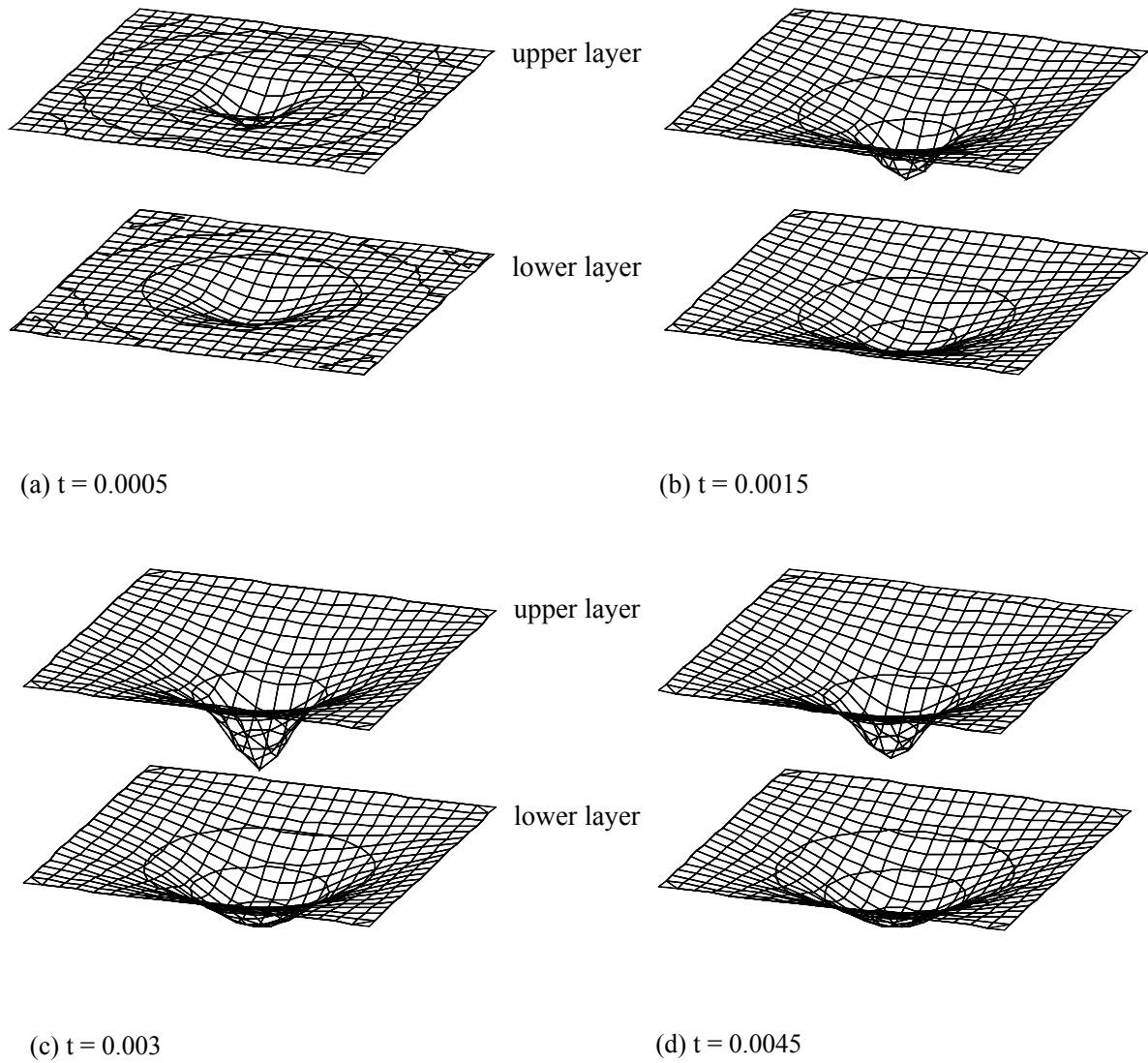


Figure 13: Deformation Configuration of the Face Layers of Sandwich Plate #1 Due to a Half Sine Shock Impulse at the Center for (a) $t=0.0005$ sec., (b) $t=0.0015$ sec., (c) $t=0.003$ sec., (d) $t=0.0045$ sec

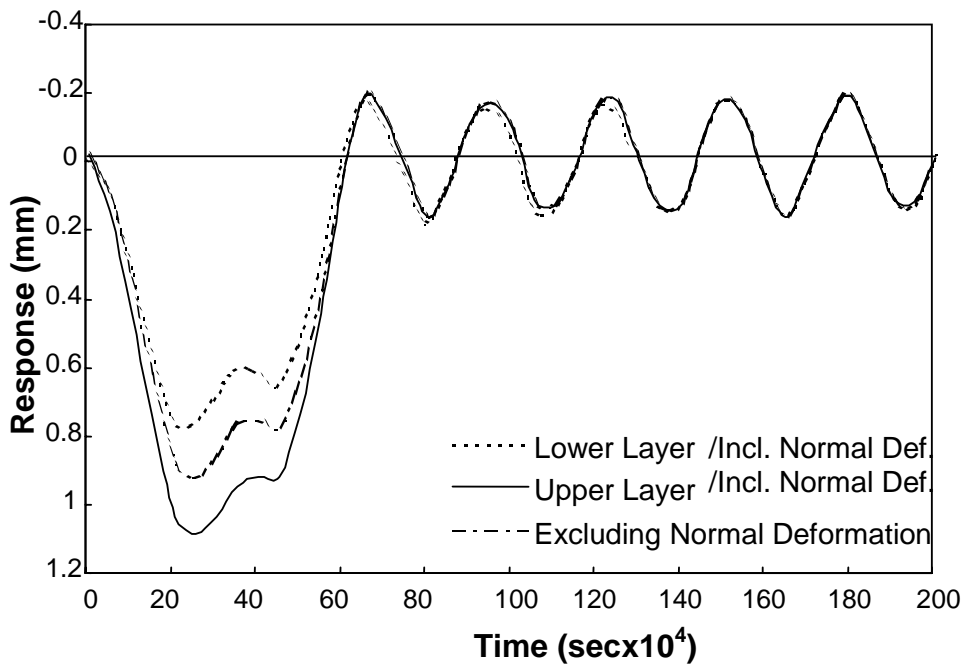


Figure 14: Time-history of Shock Response of the Face Layers of Sandwich Plate #1 Due to Point Loading at the Center, Including and Excluding Normal Deformation in the Core (ϵ_z)

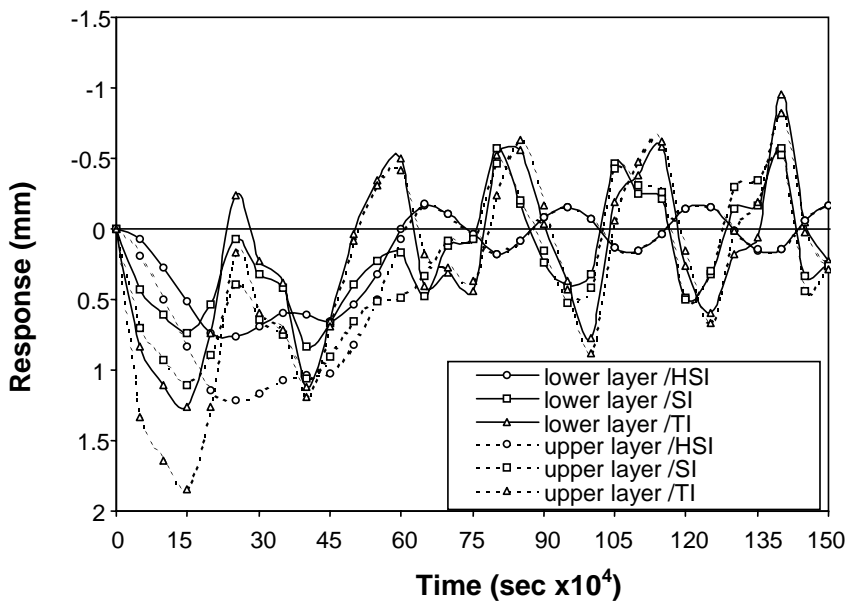


Figure 15: Time-history of Shock Response of Sandwich Plate #1 Due to Point Loading at the Center for Different Types of Impact Loading

REFERENCES

- Bottega, W.J. 1988. An Axi-symmetric Solution for the Transient Problem of a Multilayered Elastic Solid of Finite Extent, *Mechanics Research Communications*, 15: 11-20.
- Grover, A.S. and Kapur, A.D. 1982. Shock Response of Viscoelastically Damped Sandwich Plates, *Journal of Sound and Vibration*, 85: 355-364.
- He, J.F. and Ma, B.A. 1988. Analysis of Flexural Vibration of Viscoelastically Damped Sandwich Plates, *Journal of Sound and Vibration*, 120: 20-37.
- Hoff, N.J. 1950. Bending and Buckling of Rectangular Sandwich Plates, *National Advisory Committee for Aeronautics (NACA)*, TN-2225.
- Koller, M.G. 1986. Elastic Impact of Spheres on Sandwich Plates, *Journal of Applied Mathematics and Physics (ZAMP)*, 37: 256-269.
- Lange, K.A. and Bottega, W.J. 1998. On the Elastodynamic Response of Thick Multilayered Plates Subjected to Impact Loads, *Journal of Sound and Vibration*, 211:39-93.
- Lee, L.J., Hunge, K.Y. and Fann, Y.J. 1993. Dynamic Response of Composite Sandwich Plates Impacted by Rigid Ball, *Journal of Composite Materials*, 27: 1238-1256.
- Lee, B.C. and Kim, K.J. 1997. Effects of Normal Strain in Core Material on Modal Property of Sandwich Plates, *Journal of Vibration and Acoustics*, 119: 493-503.
- Paz, Mario. 1980. Structural Dynamics Theory and Computation. Van Nostrand Reinhold Company, New York.
- Poltorak, K. and Nagaya, K. 1986. A Method for Solving Forced Vibration Problems of Arbitrary Shaped Sandwich Plates, *Journal of Acoustical Society of America*, 80: 1408-1413.
- Sayir, M. and Koller, M.G. 1986. Dynamic Behavior of Sandwich Plates, *Journal of Applied Mathematics and Physics (ZAMP)*, 37: 78-103.
- Yan, M.J. and Dowell, E.H. 1972. Governing Equations for Vibrating Constrained-Layer Damping Sandwich Plates and Beams, *Journal of Applied Mechanics*, 1041-1046.